

Application of Molecular Simulation Technique To Calculate Structure and Define Deformation Mechanisms of High-Performance Polymers

Xiaozhen Yang and Shaw Ling Hsu*

Polymer Science and Engineering Department, University of Massachusetts, Amherst, Massachusetts 01003

Received May 20, 1991; Revised Manuscript Received August 8, 1991

ABSTRACT: Calculations of some properties of the crystalline unit cells of polyethylene, poly(*p*-phenylene terephthalamide), and poly(*p*-benzamide) are reported. The computed deformation behavior of these polymers is described. Computed diffraction patterns calculated for simulated structures of poly(*p*-phenylene terephthalamide) and poly(*p*-benzamide) were useful in defining the relative placement of hydrogen-bonded sheets. The calculated moduli, both parallel and perpendicular to the chain axis, for the three model polymers studied, agree well with experimental values available. Poly(*p*-phenylene terephthalamide) and poly(*p*-benzamide) contain unit cells with strong interchain interactions, and significant differences were found in calculated longitudinal moduli for the full three-dimensional calculation versus the single-chain approximation used in earlier studies. Secondary interactions, in fact, raised the longitudinal moduli to the 300-GPa range when interchain interactions such as hydrogen bonds were explicitly considered. Molecular simulation also provides information concerning perturbative effects of strong interchain interactions on deformation mechanisms.

Introduction

The elastic constant derived from the stress-strain curve for crystalline polymers is often used as a measure of mechanical performance. Because of sample heterogeneity, even for ultradrawn fibers, however, much of the sample deformation is dominated by the behavior of the amorphous phase. The true response of the crystalline phase is often difficult to obtain. In some instances, Young's modulus along the chain can be reliably obtained by Brillouin, Raman, or neutron-scattering spectroscopy methods.¹⁻⁵ By eliminating or minimizing amorphous strain, X-ray diffraction can also be used to measure the elastic constant along the chain.⁶ For applications such as finite element analysis, a full set of nine elastic constants, in addition to the generally available longitudinal modulus and Poisson's ratio, is required. Surprisingly, wood is perhaps the most completely defined anisotropic material.⁷ Therefore, in calculations needing all nine elastic constants, the anisotropic behavior of polymer fibers is therefore scaled to the ones known for wood. To obtain a complete mechanical property evaluation, many have resorted to theoretical calculations. In this spirit, molecular simulation computations are used in the work reported here to generate the crystalline unit cell for three polymers: polyethylene (PE), poly(*p*-phenylene terephthalamide) (PPTA), and poly(*p*-benzamide) (PBA). PE was analyzed due to the availability of extensive experimental and theoretical values in order to validate our simulation procedure. PPTA and PBA were selected to represent polymers with strong interchain interactions, such as hydrogen bonds. It proved possible to obtain a full set of elastic constants from simulated deformation experiments. By use of these results, the deformation behavior of these polymers was analyzed under longitudinal and shear stress.

Mechanical properties can be obtained in several ways. Based on force constants derived from normal coordinate analysis of vibrational spectra, Young's moduli of some polymers have been calculated.^{3,4,8-14} Since most vibrational spectra are analyzed using single-chain approxi-

mations, accurate estimates for three-dimensional crystals are difficult to obtain. Other studies have been carried out using programs developed in various laboratories.¹⁵⁻¹⁸ Commercial softwares are used in the work reported here together with analysis programs developed in our laboratory.

The present study on the three high-performance polymers can be divided into two parts: (1) prediction of crystalline structure and (2) characterization of deformation mechanisms. Even though PE has been studied previously,^{17,18} the first aspect should still be carried out in order to validate our simulation technique. Recently, simulation studies using a totally different approach have been reported.^{15,16} We intend to compare our calculated structures with this earlier study. A full set of elastic constants are then derived from simulated deformation experiments. Crystalline unit cells for PE, PPTA, and PBA, as well as an analysis of the diffraction patterns, have been determined. Deformation behavior under longitudinal and shear stress are then analyzed. The molecular simulation technique, incorporating both interchain and intrachain contributions, has provided new insight into deformation mechanisms.

Molecular Simulation and Method

Simulations of the crystal structures and properties of PE, PBA, and PPTA were done with the programs POLYGRAF and CERIU (Molecular Simulations Inc., Sunnyvale, CA) using the Dreiding force field described earlier.¹⁹ The intramolecular force field contained contributions from bond stretching, valence angle bending, torsional, and inversion terms. Nonbonded secondary interactions included van der Waals, electrostatic, and hydrogen-bonded terms. A cutoff distance of 9 Å was established for the van der Waals terms in order to reduce cumulation of roundoff error and to improve the speed of computation. The Ewald method was used to include the long-range effects of electrostatic interaction.²⁰ Two Silicon Graphics SD-25 Personal Iris computers were used to carry out all the calculations described here. Because periodic boundary conditions were used, the number of atoms considered is rather small. Therefore, the computation time required for energy minimization even for the most complex of the three model polymers, PPTA, was generally less than 14 h.

* To whom correspondence should be addressed.

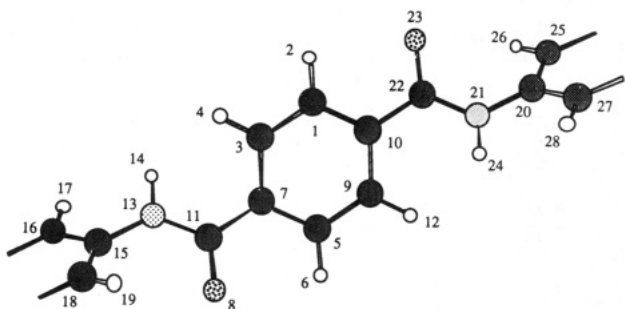


Figure 1. Calculated structure of PPTA. The atom numbering scheme is used to define structural parameters shown in Table I.

Unlike polyethylene, a number of polar groups occur along the backbone of PBA and PPTA. Interactions between these polar groups are needed to simulate a chain properly, including electrostatic terms and hydrogen bonding. Two methods were used to calculate partial charges for each atom.^{21,22} The conventional method is to calculate partial charges on each atom and then to include Coulombic electrostatic interactions between these charges. In some instances, structural calculations without charges may be more appropriate as nonbonded energy parameters in the force field include contributions from some of the electrostatic interactions.¹⁹ The hydrogen-bonded terms, however, must be carefully considered independently.¹⁹

The bulk crystalline state is simulated by use of the periodic boundary condition; i.e., polymer chains are packed into a unit cell and the cell is infinitely repeated in a three-dimensional space. This method permits study of an infinite system, eliminating perturbations from end groups and incorporating both nonbonded intermolecular and intramolecular interactions. The unit cell has been characterized for each of the three model polymers studied. Even without having all observed spacings assigned in PPTA or PBA, the number of chains in the unit cell and unit cell symmetry has been postulated.²³⁻²⁵ The diffraction pattern for each polymer is obtained using CERIUS. Diffraction patterns for both powders and oriented fibers can be generated and compared to experimental data.

Generation of a correct unit cell normally necessitates a downward scaling of the van der Waals radii of the atoms. A scaling factor of 0.3 was chosen for the initial calculation; i.e., the van der Waals radii for polymer packing is 30% of the full value. The van der Waals radii were returned to full value upon completion of packing. The structures were minimized until the energy change was smaller than 0.001 kcal/mol. Energy minimization (molecular mechanics) and molecular dynamics were used alternately for each initial structure. Only the structure with the lowest energy over many runs was further analyzed. Simulation of PPTA and PBA using a single-chain approximation was first carried out. The full unit cell containing two chains was then constructed from this single-chain approximation. The energy of the entire unit cell was then minimized. PPTA and PE structures have been studied by diffraction previously. In contrast, despite the many similarities between PPTA and PBA, very little structural characterization has been carried out for PBA. The single-chain structure of PPTA and atoms used to define structural parameters are shown in Figure 1. The structural parameters of PBA and PPTA derived from simulation technique are shown in Table I. Crystalline structures of PPTA and PBA are shown in Figures 2 and 3. In these figures, only the unit cell is shown. Because of the periodic boundary condition, this motif is surrounded by 26 similar cells. To calculate elastic constants, a strain along a particular plane or a stress on any plane associated with the unit cell was induced. The entire structure was then minimized under this constraint. The values obtained were then used to calculate the elastic constants. Decomposition of the total potential energy into various intramolecular and intermolecular terms can be obtained from the output. The simplest approach to approximate single-chain behavior is to extend the lateral dimension of the cell until virtually all interchain interactions are eliminated.

Results and Discussion

In order to validate the simulation procedure followed in our study, the unit cells for the three polymers, PE, PPTA, and PBA, were simulated and analyzed. The unit cell dimensions are summarized in Table II. For PE, the repeat along the chain was accurately calculated (1.18% error) as compared to the measured values obtained for the crystalline linear sample. The maximum deviation is along the *b* axis at 4.04%. A setting angle of 41° was obtained. This value agrees well with the limited experimental data available.²⁶ It should be pointed out, however, that the calculated value represents the structure at absolute zero. Unit cell parameters calculated for the strongly hydrogen bonded systems PPTA and PBA are most accurate for the *c* axis repeat (0.6% or 1.25%) and least accurate for the stacking distance of hydrogen-bonded planes in PPTA, with a maximum error of 5.97%. Repeats containing interchain hydrogen-bonded sheets are accurately simulated.

The details regarding PPTA and PBA three-dimensional structures are extremely interesting. It is important to compare the calculated structures to those derived from diffraction data. In PPTA, the dihedral angle obtained for the adjacent phenyl rings is ~72°. An angle of -33° between the amide plane and the terephthalic segment was calculated. This is somewhat larger than the -30° found experimentally. The angle between the amide plane and the phenylene plane is 37°, which compares favorably to the 38° measured.²¹ A detailed comparison of some of the structural parameters, including hydrogen bond length, derived using other simulation techniques and force fields together with experimental values is shown in Table III. The general agreement between the present calculation and the previous one is good. Both calculations also agree well with experimental data.

Diffraction patterns calculated using CERIUS reproduce remarkably well those obtained experimentally. The pattern of an oriented PPTA fiber is shown in Figure 4. This pattern was generated by assuming the average angular deviation between the chain axis with respect to the deformation axis to be 5°. This is equivalent to a nearly perfectly oriented axis with an orientation function of 0.99. The most remarkable difference between the simulated and experimental pattern is the intensity of (001) spacings. In many of the observed diffraction patterns, the (001) spacings are extremely weak, especially for samples annealed at high temperature and under tension. By translating the central chain, or equivalently by moving the hydrogen-bonded planes relative to each other, the calculated intensity of the (001) spacings can be made to vary significantly. In the simulated diffraction pattern, the equilibrium structure corresponds to one with hydrogen-bonded sheets displaced relative to one another along the chain axis by nearly 1 Å with great loss in the (001) intensity. For PPTA and other liquid-crystalline rodlike polymers, annealing at elevated temperatures and under tension was required in order to observe well-characterized diffraction patterns.^{7,27} It should also be noted that this annealing procedure is necessary to produce fibers of high modulus and strength, and presumably of a more ordered structure. However, for these ordered structures obtained after annealing, the (001) intensity diminished significantly,^{7,13,23} making the measured diffraction pattern virtually identical to the calculated one. Earlier experimental studies have also suggested that the structure, i.e., symmetry, of the unit cell is altered by the annealing process. The relative intensity of the (001) diffractions can only be explained by a small displacement

Table I
Definition of Structural Parameters in PPTA^a

bond length	Å	bond length	Å	bond length	Å
C(1)-H(2)	1.020	C(7)-C(5)	1.416	C(22)-N(21)	1.358
C(3)-H(4)	1.022	C(5)-C(9)	1.408	N(21)-C(20)	1.356
C(5)-H(6)	1.023	C(9)-C(10)	1.414	C(22)-O(23)	1.256
C(9)-H(12)	1.023	C(10)-C(1)	1.414	N(21)-H(24)	0.960
N(13)-H(14)	0.960	C(7)-C(11)	1.410	C(16)-H(17)	1.021
C(11)-O(8)	1.255	C(11)-N(13)	1.359	C(18)-H(19)	1.019
C(1)-C(3)	1.405	N(13)-C(15)	1.356	C(25)-H(26)	1.021
C(3)-C(7)	1.412	C(10)-C(22)	1.411	C(27)-H(28)	1.023

bond angle	deg	torsion angle	deg
H(2)-C(1)-C(3)	118.279	H(2)-C(1)-C(3)-C(7)	-179.684
H(4)-C(3)-C(7)	120.640	H(4)-C(3)-C(1)-C(10)	179.294
H(6)-C(5)-C(9)	118.459	H(6)-C(5)-C(9)-C(10)	179.453
H(12)-C(9)-C(10)	120.470	H(12)-C(9)-C(5)-C(7)	-179.294
C(3)-C(7)-C(11)	120.912	C(1)-C(3)-C(7)-C(5)	-0.633
C(9)-C(10)-C(22)	121.610	C(3)-C(7)-C(5)-C(9)	0.838
C(10)-C(1)-C(3)	121.386	C(7)-C(5)-C(9)-C(10)	-0.448
C(1)-C(3)-C(7)	121.012	C(5)-C(9)-C(10)-C(1)	0.000
C(3)-C(7)-C(5)	117.758	C(9)-C(10)-C(1)-C(3)	0.316
C(7)-C(5)-C(9)	121.192	C(5)-C(7)-C(11)-N(13)	-147.081
C(5)-C(9)-C(10)	120.975	C(7)-C(11)-N(13)-C(15)	-175.512
C(9)-C(10)-C(1)	117.678	C(11)-N(13)-C(15)-C(16)	-144.929
C(7)-C(11)-N(13)	121.045	C(1)-C(10)-C(22)-N(21)	148.043
C(10)-C(22)-N(21)	120.981	C(10)-C(22)-N(21)-C(20)	175.024
O(8)-C(11)-N(13)	120.507	C(22)-N(21)-C(20)-C(27)	144.171
O(23)-C(22)-N(21)	120.433	O(8)-C(11)-N(13)-H(14)	-170.994
C(11)-N(13)-C(15)	128.038	O(23)-C(22)-N(21)-H(24)	170.410
C(22)-N(21)-C(20)	127.747	H(17)-C(16)-C(15)-C(18)	179.368
C(16)-C(15)-C(18)	118.503	H(19)-C(18)-C(15)-C(16)	-178.268
C(25)-C(20)-C(27)	118.620	H(26)-C(25)-C(20)-C(27)	178.387
C(13)-C(15)-C(16)	117.611	H(28)-C(27)-C(20)-C(25)	-180.000
C(21)-C(20)-C(27)	117.459		

^aThe atom numbers correspond to the structure shown in Figure 1.

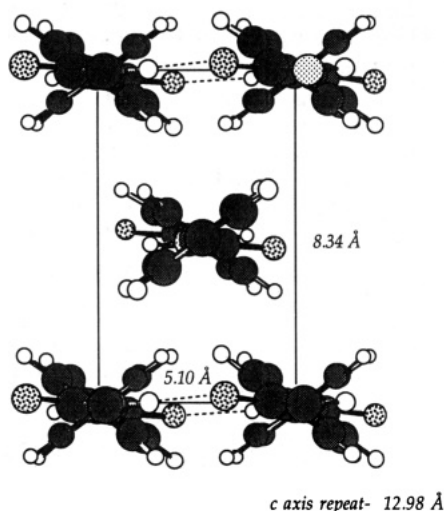


Figure 2. Unit cell calculated for PPTA.

(~ 0.35 Å) of the two chains in the unit cell.²³ Although the exact magnitude of the shift is uncertain, these earlier experimental data are consistent with our calculated results. A single chain of PBA is known to have a 2-fold symmetry with structural parameters very similar to PPTA. The chains are packed in an orthorhombic unit cell.

The accuracy of the calculated equilibrium structures is determined by the accuracy of the potential energy of the system. Both for systems involving only van der Waals forces (PE) and for systems containing strong specific secondary forces (PBA and PPTA), reasonable crystal structures can be predicted. This result provides a much higher level of confidence of the elastic constants calculated for each system. Because of differences in various atom-

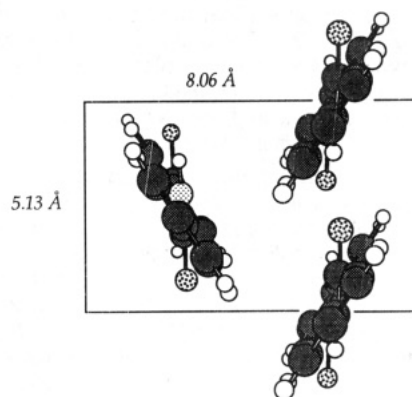


Figure 3. Unit cell calculated for PBA.

atom interactions, anisotropic features must exist, unless crystalline units have very high symmetry. This situation is especially true for polymers, because covalent bonds along the chain are much stronger than nonbonded secondary interchain interactions. The number of elastic constants to be calculated is 21 for a crystalline state with only translational repeats, i.e., one that is isomorphic to a triclinic unit cell. There are 13, 9, 5 and 3 linearly independent constants for monoclinic, orthorhombic, hexagonal, and cubic symmetries, respectively. As mentioned previously, very few of these elastic constants are well characterized for polymer crystallites. Most earlier studies concentrated on the elastic constant, G_{zz} , along the chain axis. Shear moduli G_{xx} or G_{zy} are available only for the simplest system, polyethylene.^{18,28}

Each of the polymers examined should have nine independent elastic constants, consistent with the unit cell spatial symmetry associated with PE and PBA, or PPTA. The calculated values are listed in Table IV. The longitudinal modulus calculated for PE is 298 GPa, slightly

Table II
Geometric Parameters (Å) of the Unit Cell Calculated for the Model Polymers

	PPTA			PBA			PE		
	calc	obs	error, %	calc	obs	error, %	calc	obs	error, %
<i>a</i>	8.34	7.87	5.97	8.06	7.71	4.54	7.21	7.42	-2.83
<i>b</i>	5.01	5.19	-3.47	5.13	5.14	-0.19	5.15	4.95	4.04
<i>c</i>	12.98	12.9	0.60	12.96	12.8	1.25	2.58	2.55	1.10
ρ	1.46	1.49	-2.01	1.48	1.48	0.00	0.97	0.98	-1.02

Table III
Calculated and Observed Structural Parameters for PPTA

	simulated structure I ^a	simulated structure II ^b	exptl data ^c	exptl data ^d
<i>a</i> , Å	8.3	8.34	7.8	7.87
<i>b</i> , Å	5	5.0	5.19	5.18
<i>c</i> , Å	13.1	12.98	12.9	12.9
α , deg	90	90	90	90
β , deg	90	90	90	90
γ , deg	92	90	90	90
chain location	[0,0]; [1/2,1/2]	[0,0]; [1/2,1/2]	[0,0]; [1/2,1/2]	[0,0]; [1/2,1/2]
diacid ring rotation, deg	-26	-33	(~30)	-30
diamide ring rotation, deg	43	37	(~30)	38
density, g/cm ³	1.45	1.46	1.49	1.48
H-bond length, Å	2.3	1.97		2.1
angle of N-H...O, deg	160	173		160
distance of N...O, Å		2.93		3.04

^a Rutledge, G. C.; Suter, U. W.; Papaspyrides, C. D. *Macromolecules* 1991, 24, 1934. ^b This study. ^c Tashiro, K.; Kobayashi, M.; Tadokoro, H. *Macromolecules* 1977, 10, 413. ^d Northolt, M. G. *Eur. Polym. J.* 1974, 10, 799.

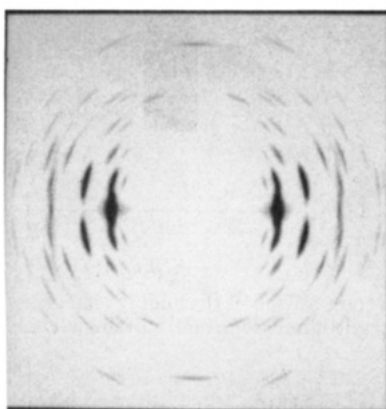


Figure 4. X-ray diffraction pattern simulated for a highly oriented PPTA fiber. The angular deviation is 5° or equivalent to an orientation function of 0.99.

Table IV
Elastic Constants (GPa) Calculated for the Three Model Polymers

	PPTA	PBA	PE
E_x	14.9	12.8	10.7
E_y	80.1	60.8	8.4
E_z	335.7	322.3	297.5
G_{yz}	15.4	14	3.7
G_{zx}	0.7	0.9	1.5
G_{xy}	5.2	8.9	8.3
μ_{xy}	0.199	0.259	0.215
μ_{zx}	0.496	0.331	0.025
μ_{yz}	0.717	0.872	0.472

higher than the 290 GPa obtained from Raman or neutron-scattering spectroscopy experiments.¹⁻⁵ The transverse elastic constants are ~10 GPa, somewhat lower than the values of 13–16 GPa measured for *n*-alkanes.²⁹⁻³¹ The shear moduli of PE, G_{yz} and G_{zx} were found to be 5.0 and 2.4 GPa, respectively, in comparison to the 3.7 and 1.5 GPa found in an earlier calculation.²⁸ As seen from energy decomposition analysis, intramolecular bond stretching and valence angle deformation terms dominate when PE is deformed along the chain axis, as expected. When sheared, van der Waals forces dominate, as shown in Figure

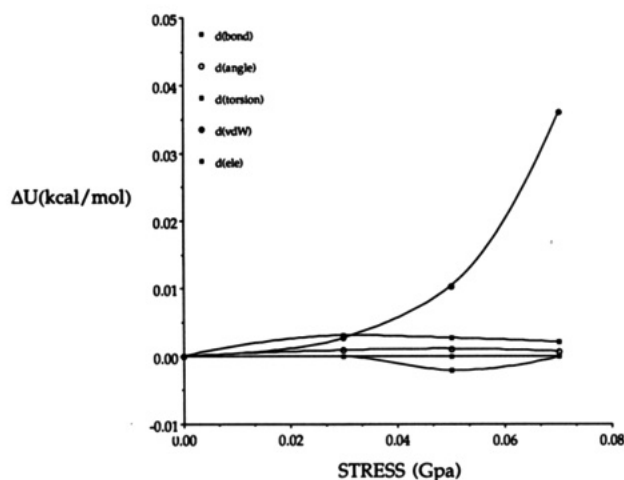


Figure 5. Relative contribution of various secondary energy terms for PE under shear stress.

5. These results are consistent with the planar zigzag structure of PE. The potential energy distribution is comparable with values derived earlier from single-chain analysis.⁵

Analysis of PPTA and PBA presents an interesting evaluation of molecular simulation. In general, the calculated values are higher than those obtained experimentally. For example, a value of 335 GPa was obtained for PPTA, whereas the experimental value is 153 GPa.⁶ A number of factors, including degree of crystallinity, segmental orientation, lattice distortion, or packing defects, can lower the experimental longitudinal modulus.³² As mentioned earlier, postprocessing treatment can markedly improve mechanical properties.^{7,27} Surprisingly, the values calculated in this work are considerably higher than those previously calculated using a single-chain approximation. For PE, the deformation behavior of the unit cell is not significantly different for the single-chain approximation. For PPTA deformed longitudinally, most of the strain is divided into contributions from the bonds and valence angles, as displayed in Figure 6. However,

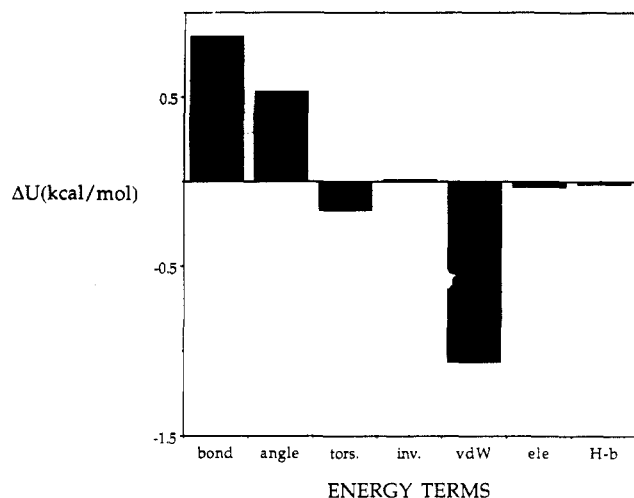


Figure 6. Relative contribution of various secondary energy terms for PPTA deformed longitudinally.

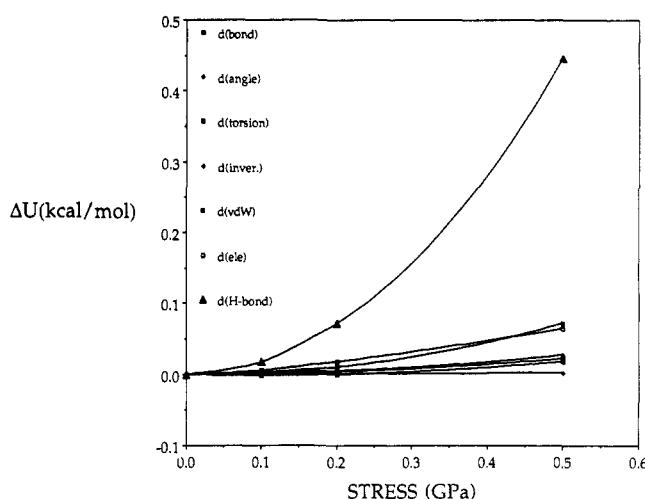


Figure 7. Deformation behavior of PPTA under shear stress.

when PPTA crystals are sheared, strongly hydrogen bonded interactions dominate the restoring force, as shown in Figure 7. It is of interest to note the small value of the stress needed to move hydrogen-bonded sheets relative to each other.

The least studied of the three polymers in this analysis is PBA. The chain conformation of this polymer differs considerably from that of PPTA.¹³ For the full unit cell calculation, the modulus along the chain was found to be 322 GPa. The decomposition of the energy is shown in Figure 8; intramolecular bond stretching, valence angle bending, and van der Waals and hydrogen bonding are all important. Upon elimination of interchain interactions and reversion to a single-chain approximation, a completely different deformation mechanism was found. For this approximation without interchain interactions, the torsional term became dominant, as shown in Figure 9. This result clearly illustrates the importance of intermolecular interactions. Incorporating those terms severely restricts the degree of freedom associated with valence angle bending or torsional motions. Most of the strain is then absorbed by bond deformation, and this raises the longitudinal modulus to a considerably higher value than is predicted by the single-chain approximation.

Conclusions

The molecular simulation technique has been successfully used to calculate structures of polymers with or

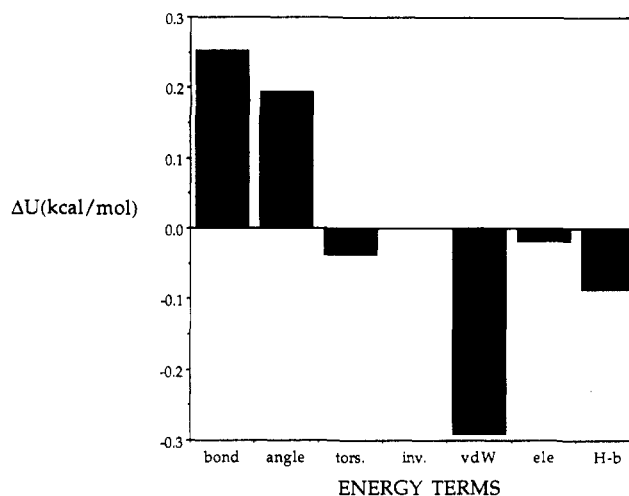


Figure 8. Energetics of PBA under longitudinal stress.

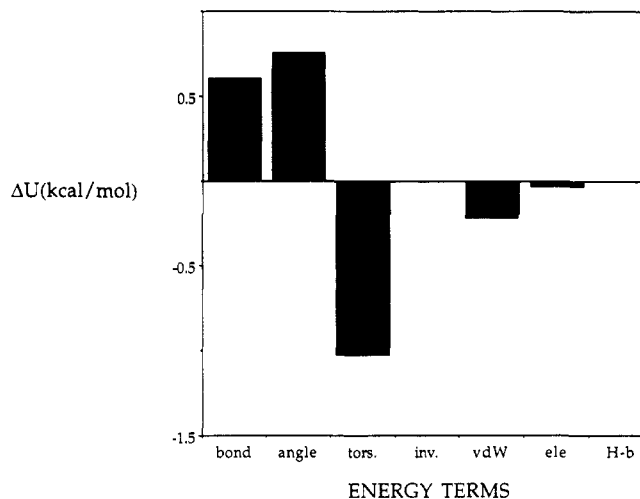


Figure 9. Decomposition of the energy change associated with PBA under longitudinal deformation: single-chain approximation.

without strong specific interchain interactions. The calculated unit cell parameters compared favorably with experimental data. The elastic constants obtained using the three-dimensional unit cells are consistently higher than expected for the single-chain approximation. The simulated deformation behavior of PPTA is consistent with our expectation because strong specific hydrogen-bonded interactions dominate the stability of the three-dimensional structure. A most interesting case is the bent PBA molecule. The deformation mechanism in the single-chain approximation was found to differ considerably from that in the full three-dimensional model. Due to the hydrogen bonding, angle bending or bond rotation is severely limited, and this raises the longitudinal modulus much higher than is predicted by the single-chain approximation.

References and Notes

- (1) Strobl, G. R.; Eckel, R. *J. Polym. Sci., Polym. Phys. Ed.* **1976**, *14*, 913.
- (2) Holiday, L.; White, J. W. *Pure Appl. Chem.* **1971**, *26*, 545.
- (3) Kim, P.; Chang, C.; Hsu, S. L. *Polymer* **1987**, *27*, 34.
- (4) Yang, X.; Chian, R.; Hsu, S. L. *Preprints, National Symposium on Molecular Spectroscopy*; Hainan, 1988; p 77.
- (5) Hsu, S. L.; Krimm, S. *J. Appl. Phys.* **1976**, *47*, 4265.
- (6) Sakurada, I.; Kaji, K. *J. Polym. Sci., Part C* **1970**, *31*, 57.
- (7) Allen, S. R. Ph.D. Thesis, University of Massachusetts, Amherst, MA, 1983, and references therein.
- (8) Meyer, K. H.; Lotmar, W. *Helv. Chim. Acta* **1935**, *19*, 68.

- (9) Mark, H. *Trans. Faraday Soc.* **1936**, *32*, 144.
- (10) Treloar, L. R. G. *Polymer* **1960**, *1*, 95, 279, 290.
- (11) Shimanouchi, T.; Asahina, M.; Enomoto, S. *J. Polym. Sci.* **1962**, *59*, 93.
- (12) Miyazawa, T. *Rep. Prog. Polym. Phys. Jpn.* **1965**, *8*, 47.
- (13) Tashiro, K.; Kobayashi, M.; Tadokoro, H. *Macromolecules* **1977**, *10*, 413.
- (14) Brown, D.; Clarke, J. H. R. *J. Chem. Phys.* **1986**, *84*, 2858.
- (15) Rutledge, G. C.; Suter, U. W. *Macromolecules* **1991**, *24*, 1921.
- (16) Rutledge, G. C.; Suter, U. W.; Papaspyrides, C. D. *Macromolecules* **1991**, *24*, 1934.
- (17) Sorensen, R. A.; Liao, W. B.; Boyd, R. H. *Macromolecules* **1988**, *21*, 194.
- (18) Sorensen, R. A.; Liao, W. B.; Kesner, L.; Boyd, R. H. *Macromolecules* **1988**, *21*, 200.
- (19) Mayo, S. L.; Olafson, B. D.; Goddard, W. A., III *J. Phys. Chem.* **1990**, *94*, 8897.
- (20) De Leuw, S. W.; Perram, J. W.; Smith, E. R. *Proc. R. Soc. London* **1980**, *A373*, 27.
- (21) Gasteiger, J.; Marsili, M. *Tetrahedron* **1980**, *36*, 3219.
- (22) Rappe, A. K.; Goddard, W. A. *J. Phys. Chem.*, in press.
- (23) Northolt, M. G. *Eur. Polym. J.* **1974**, *10*, 799.
- (24) Tadokoro, H. *Structure of Crystalline Polymers*; Wiley: New York, 1979.
- (25) Haraguchi, K.; Kajiyama, T.; Takayanagi, M. *J. Appl. Polym. Sci.* **1979**, *23*, 915.
- (26) Kavesh, S.; Schultz, J. M. *J. Polym. Sci., Part A-2* **1970**, *8*, 243.
- (27) Kwolek, S. L.; Morgan, P. W.; Schaefer, J. R.; Gulrich, L. W. *Macromolecules* **1977**, *10*, 1390.
- (28) McCullough, R. L.; Peterson, J. M. *J. Appl. Phys.* **1973**, *44*, 1224.
- (29) Odajima, A.; Maeda, T. *J. Polym. Sci., Part C* **1966**, *15*, 55.
- (30) Williams, D. E. *J. Chem. Phys.* **1967**, *47*, 4680.
- (31) Wobser, C.; Blasenbrey, S. *Kolloid-Z. Z. Polym.* **1970**, *241*, 985.
- (32) Morgan, R. J.; Pruneda, C. O.; Steele, W. J. *J. Polym. Sci., Polym. Phys. Ed.* **1983**, *21*, 1757.

Registry No. PE (homopolymer), 9002-88-4; PPTA (copolymer), 25035-37-4; PPTA (SRU), 24938-64-5; PBA (homopolymer), 25136-77-0; PBA (SRU), 24991-08-0.